ELSEVIER

Fuel 81 (2002) 2177–2190

FUEL

www.fuelfirst.com

Pt–WO_3 supported on carbon nanotubes as possible anodes for direct methanol fuel cells☆

B. Rajesh[a], V. Karthik[a], S. Karthikeyan[a], K. Ravindranathan Thampi[b], J.-M. Bonard[c], B. Viswanathan[a,*]

[a]*Department of Chemistry, Indian Institute of Technology, Madras, Chennai 600 036, India*
[b]*Laboratoire de Photonique et Interfaces, Ecole Polytechnique Federale de Lausanne,CH-1015 Lausanne, Switzerland*
[c]*Department de Physique, Ecole Polytechnique Federale de Lausanne, CH-1015 Lausanne, Switzerland*

Received 10 December 2001; revised 22 February 2002; accepted 23 February 2002; available online 9 July 2002

Abstract

The carbon nanotube (CNT) synthesised by the template carbonisation of polypyrrole on alumina membrane has been used as the support for Pt–WO_3, Pt–Ru, and Pt. These materials have been used as the electrodes for methanol oxidation in acid medium in comparison with E-TEK 20 wt% Pt and Pt–Ru on Vulcan XC72R carbon. The higher electrochemical surface of the carbon nanotube (as evaluated by cyclic voltammetry) has been effectively used to disperse the catalytic particles. The morphology of the supported and unsupported CNT has been characterised by scanning electron micrograph and high-resolution transmission electron micrograph. The particle size of Pt, Pt–Ru, and Pt–WO_3 loaded CNT was found to be 1.2, 2, and 5 nm, respectively. The X-ray photoelectron spectra indicated that Pt and Ru are in the metallic state and W is in the +VI oxidation state. The electrochemical activity of the methanol oxidation electrode has been evaluated using cyclic voltammetry. The activity and stability (evaluated from chronoamperometric response) of the electrodes for methanol oxidation follows the order: GC/CNT–Pt–WO_3–Nafion > GC/E-TEK 20% Pt–Ru/Vulcan Carbon–Nafion > GC/CNT–Pt–Nafion > GC/E-TEK 20% Pt/Vulcan carbon–Nafion > Bulk Pt. The amount of nitrogen in the CNT plays an important role as observed by the increase in activity and stability of methanol oxidation with N_2 content, probably due to the hydrophilic nature of the CNT.

Keywords: Methanol electrooxidation; Transition metal oxide; Carbon nanotubes

1. Introduction

Considerable interest has been devoted in recent years [1] to develop suitable electrode materials for methanol oxidation for the possible application in direct methanol fuel cells (DMFC). One of the major problems for the efficient conversion of methanol fuel to electric current in a DMFC is the slow methanol oxidation kinetics on the anode catalyst. This is mostly due to self-poisoning of the surface by reaction intermediates such as CO, which are formed during stepwise dehydrogenation of methanol [2]. Pt, the standard catalyst for the oxidation of small organic molecules including methanol, is rather active for the dehydrogenation step, but suffers seriously from CO poisoning. Therefore, methanol oxidation on Pt is possible only at potentials where adsorbed CO and other poisoning intermediates are effectively oxidised, leading to a significant overpotential and loss in efficiency. This problem necessitates the search for Pt based catalysts. Therefore number of other catalyst systems have been investigated for their suitability as methanol oxidation catalysts such as PtRu [3], PtSn [4], PtMo [5] or PtCo [6]. The origin of the superior activity of PtRu over other catalysts is the improved CO tolerance of the PtRu catalyst compared to the other systems. So, ternary and higher PtRu based catalysts such as PtRuOs [7] PtRuSn [8] PtRuW [9] PtRuSnW [10] or PtRuOsIr [11] have also been investigated for methanol oxidation. Another slightly different approach involved, is the use of transition metal oxides [12] along with Pt or Pt–Ru as the catalyst which were shown to have enhanced catalytic activity for methanol oxidation compared to that of Pt or Pt–Ru, but still not good enough for commercial applications. It has been proposed

* Corresponding author. Tel.: +91-44-235-1365; fax: +91-44-235-0529.
E-mail address: bviswanathan@hotmail.com (B. Viswanathan).
☆ Published first on the web via Fuelfirst.com—http://www.fuelfirst.com

0016-2361/02/$ - see front matter
PII: S0016-2361(02)00162-X

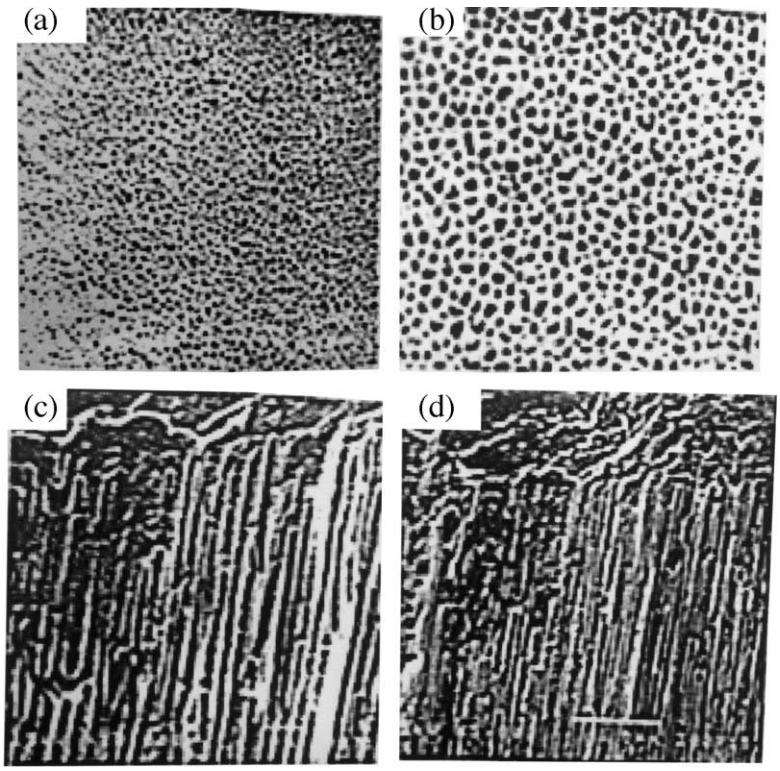

Fig. 1. Surface and cross-sectional view of alumina membrane by SEM. (a) and (b) Surface view and (c) and (d) cross-sectional view.

that the respective oxides not only increase the dehydrogenation of methanol but also have shown to be active sites for the formation of oxy species [13]. Though, Pt–WO_3 catalyst delivers higher performance and stability than pure Pt, the activity for methanol oxidation is still relatively low. The probable reason for this could be the poor utilisation of the catalyst, which is due to the larger particle size (150–200 nm) which form agglomerates [12].

In order to decrease the Pt loading and to increase the specific surface area of the catalyst, most of these materials are supported on the high surface area carbon [14]. The nature of carbon, their functionalities [15] and the method of preparation [16] of the catalyst on the carbon has pronounced effect on the electrocatalytic activity of methanol oxidation.

The discovery of carbon nanotubes by arc-discharge process (CNT) by Iijima in 1991 [17] created much excitement and stimulated extensive research into the properties of nanometer-scale cylindrical carbon networks. Carbon nanotubes are becoming technologically important materials with proposed uses ranging from nanoelectronic devices [18] to catalytic [19] for reactions such as those important in hydrogen storage materials [20] and in fuel cells [21,22]. But one of the primary challenges in the synthesis of carbon nanotubes is the control of the size, shape and the purity of the resulting carbon nanostructures. Tubular carbon materials have also been prepared by the catalytic decomposition of organic vapours such as acetylene, ethylene or propylene on catalysts such as Co [23], Ni, $LaNi_5$ [24] in an inert atmosphere and template carbonisation of polymers [25–27] and hydrocarbon [28] to circumvent some of the difficulties experienced in arc-discharge process. The template aided synthesis of carbon nanotubes and other nanomaterials takes into consideration the above-mentioned factors as the growth of nanotubes or nanoparticles is arrested due to the restricted dimensions imposed by the template. The use of template (alumina membranes) for the synthesis of the carbon nanotubes was first perfected by Martin and metal(s) filled carbon nanotubes has been used as the electrode materials for electrochemical oxidation of methanol and oxygen reduction reactions which are important in the fuel cell research [21]. Recently Bessel et al. [29] have reported methanol oxidation of Pt supported on graphite nanofibres and compared with the activity of Pt supported on Vulcan XC72 carbon. It has been shown that the Pt supported on graphite nanofibres not only exhibited higher activity but also better stability.

In order to maximise the utilisation and to increase the stability for methanol oxidation, carbon nanotubes synthesised by template method [30] has been used as the support for Pt–WO_3, Pt–Ru and Pt and these materials have been used as the electrode material for methanol oxidation in comparison with the commercially available E-TEK carbon supported 20% Pt and Pt–Ru and bulk Pt electrodes.

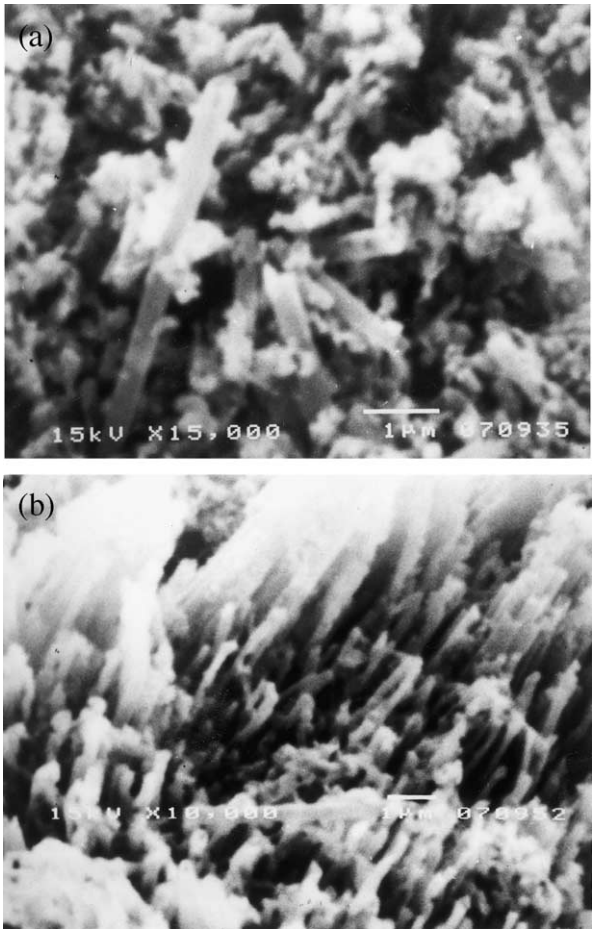

Fig. 2. SEM of carbon material obtained by carbonisation of polypyrrole for 3 h at (a) 973 K and (b) 1023 K.

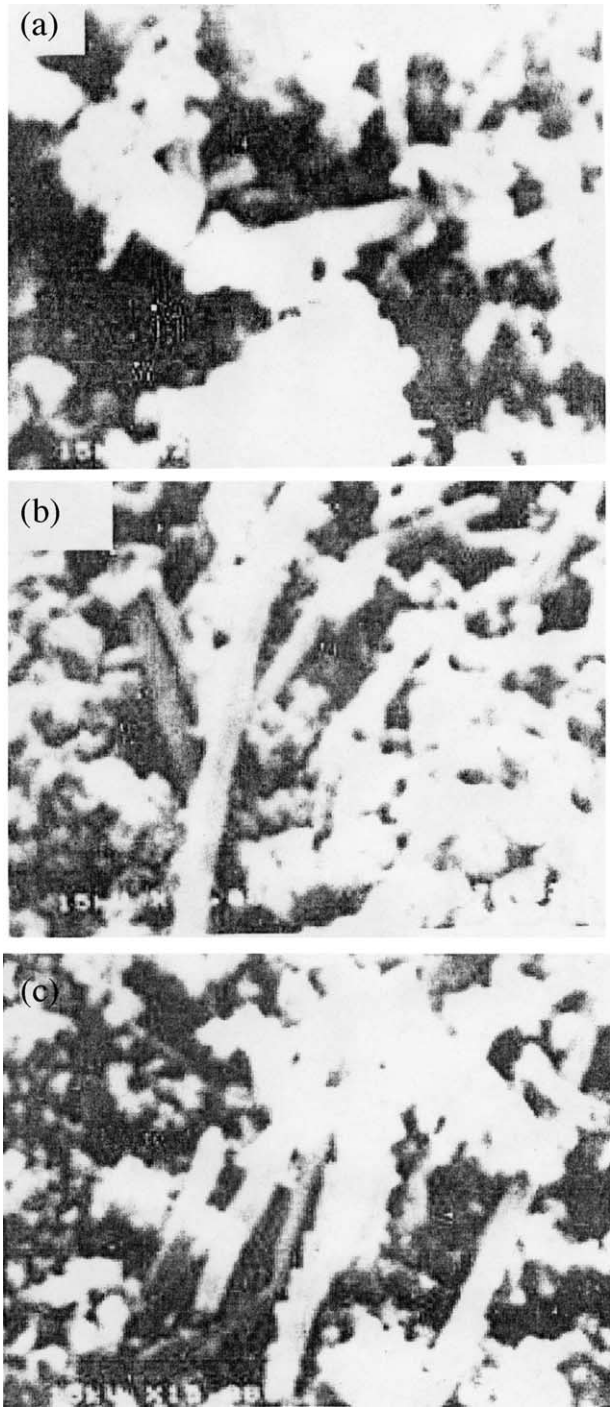

Fig. 3. SEM of carbon material obtained by carbonisation of polypyrrole at 1073 K for (a) 3 h, (b) 4 h, and (c) 5 h.

2. Experimental method

2.1. Materials

All the chemicals used were of analytical grade. Pyrrole (Sisco Research Laboratory) was distilled under vacuum prior to use. Ferric chloride hexahydrate, *p*-toluene sulphonic acid, concentrated HF, methanol, sulphuric acid, W metal powder, H_2O_2 (all from Merck) were used as received. Hexa chloro platinic acid and Ruthenium chloride were obtained from Hindustan Platinum Ltd. Nafion 5% solution (from Aldrich) was used as received. Alumina template membranes (0.2 μm pore diameter and 60 μm thick) were obtained commercially (Whatman Anopore Filters, Alltech). Glassy carbon was polished with fine alumina powder and ultrasonicated in water prior to use. 20% Pt/Vulcan carbon, Pt–Ru/Vulcan carbon catalyst was obtained from E-Tek.

2.2. Characterisation methods

Scanning electron microscopic images were obtained using JEOL 1500 microscope. The carbon nanotubes obtained after the dissolution of the template is immersed in ethanol and ultrasonicated for 20 min to disperse it completely. A drop of this suspension was placed on SEM sample holder and sputter coated with gold to prevent charging and imaged. The microscopic features of the sample were also observed with high-resolution transmission electron microscope (TEM, Philips EM430ST)

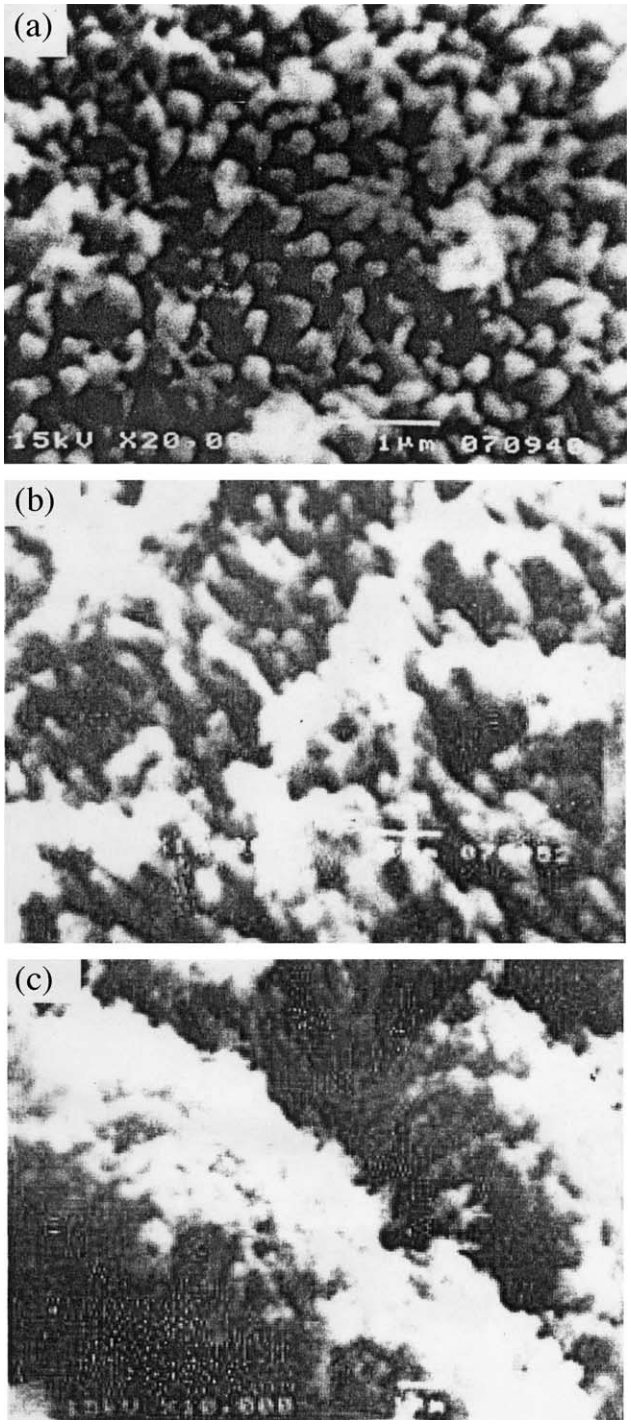

Fig. 4. SEM of tubular carbon material obtained by carbonisation of polypyrrole at 1173 K for (a) 3 h, (b) 4 h, and (c) 6 h.

operated at 300 kV. The samples were dispersed in ethanol under sonication and dropped on the carbon coated TEM grids and imaged. The X-ray photoelectron spectroscopic (XPS) measurements of nanoparticles loaded carbon nanotubes were carried out using Perkin Elmer PHI 5500 ESCA system using Mg Kα as excitation source. The elemental analysis of the CNT has been carried out using Hereaus CHN analyser. The bulk Pt on the catalyst/electrode was analysed by Inductively Coupled Plasma Atomic Emission Spectrometer (ICPAES, Model 3410, ARL) after calibration with standard solution containing known metal content. The metal was extracted from the catalyst/electrode by boiling in aqua regia.

2.3. Synthesis of carbon nanotubes

The PPy coatings were applied by a reaction coating approach by suspending alumina template membrane in an aqueous pyrrole (0.1 M) solution containing 0.2 M ferric chloride hexahydrate and slowly 0.2 M *p*-toluene sulphonic acid was added and polymerisation was carried out for 3 h. This leads to the black coating of polypyrrole on the template membrane. The surface layers were removed by polishing with fine alumina powder and ultrasonicated for 20 min to remove the residual alumina used for polishing. The membrane was then dried and placed in quartz boat and carbonised in Ar atmosphere (at different temperatures and time intervals). The resulting curled carbon/alumina composite was immersed in 48% HF for 24 h to remove the template. The residue was thoroughly washed with water to remove the HF and dried.

2.4. Loading of metal(s) nanocluster inside CNTs

Pt or PtRu nanoclusters were loaded inside the CNT as follows, the C/alumina composite obtained (before the dissolution of template membrane) was immersed in 73 mM H_2PtCl_6(aq) or in a mixture of 37 mM hexachloroplatinic acid and 73 mM ruthenium chloride for 12 h. After immersion the membrane was dried in air and the ions were reduced to the corresponding metal(s) by a 3 h exposure to flowing H_2 gas at 823 K. The underlying alumina was then dissolved by immersing the composite in 48% HF for 24 h. The membrane was removed from the HF solution and treated in the same way as for unloaded CNT to remove residual HF. These processes result in Pt or Pt–Ru nanocluster loaded CNT.

2.5. Loading of WO_3 inside carbon nanotubes

The carbon/Alumina composite was immersed in peroxo-tungstic acid solution (obtained by dissolving W metal powder in 30% H_2O_2, followed by the decomposition of excess H_2O_2 using platinised platinum and the concentration of peroxo-tungstic acid with respect to W was 0.1 M) between 24 and 48 h. The material was ultrasonicated for 5 min to remove any precipitate which is formed on the composite (polymeric form of tungsten oxides may be precipitated on prolonged standing). The immersion leads to the penetration of peroxo-tungstic acid inside the pores of composite. The composite was then dried in air at room temperature for 1 h and heated at 723 K for 4 h, which results in the formation of WO_3. The WO_3 incorporated

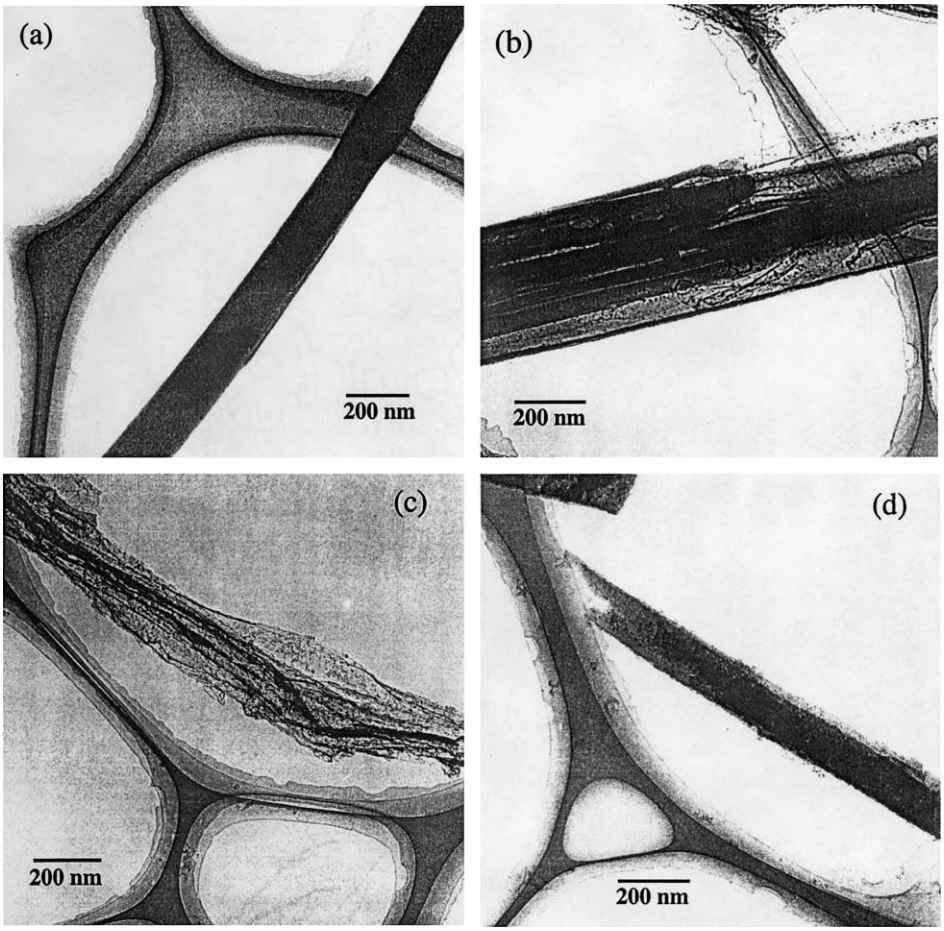

Fig. 5. HR-TEM images of carbon nanotube obtained by the carbonisation of polypyrrole at 1173 K for (a) and (b) 3 h and (c) and (d) 6 h.

carbon nanotube (WO_3/CNT) was collected by dissolving the template (Alumina membrane) in 48% HF for 24 h. The residue was completely washed with de-ionised water several times to remove the HF.

2.6. Loading of Pt/WO_3 inside carbon nanotube

The WO_3/Carbon/Alumina composite was immersed in 73 mM H_2PtCl_6 for 48 h dried and reduced at 623 K for 4 h in H_2 atm. The alumina membrane was dissolved in 48% HF for 24 h. It was then repeatedly washed with de-ionised water to remove HF, dried in air at 333 K to obtain Pt/WO_3 incorporated CNT.

2.7. Preparation of composite electrodes

The electrodes for the electrochemical measurements were fabricated by dispersing the unloaded or loaded CNT (after the template removal) in 200 μl of deionised water and 25 μl of 5 wt% Nafion solution was then added and ultrasonicated for 20 min. A known amount of suspension was added on to the glassy carbon (GC) electrode and solvent was slowly evaporated which results in unloaded or loaded GC/CNT–Nafion composite electrode.

2.8. Electrocatalytic measurements

Electrocatalytic measurements were made with Wenking potentio scan (POS73) with digital 2000 $X-Y$ recorder. Three electrodes cell consisting of the Glassy Carbon (0.07 cm^2) working electrode, Pt foil (1 cm^2) counter electrode and Ag/AgCl electrode as the reference electrode was used, respectively. The H_2SO_4 and CH_3OH was used as the electrolyte and polariser, respectively. The stability of the electrodes was evaluated from current–time plot by polarising the electrode at particular potential with respect to time in 1 M H_2SO_4 and 1 M CH_3OH.

3. Results and discussion

3.1. Morphological characterisation by SEM

The surface and cross-sectional view of the alumina membrane (pore diameter 200 nm) are shown in

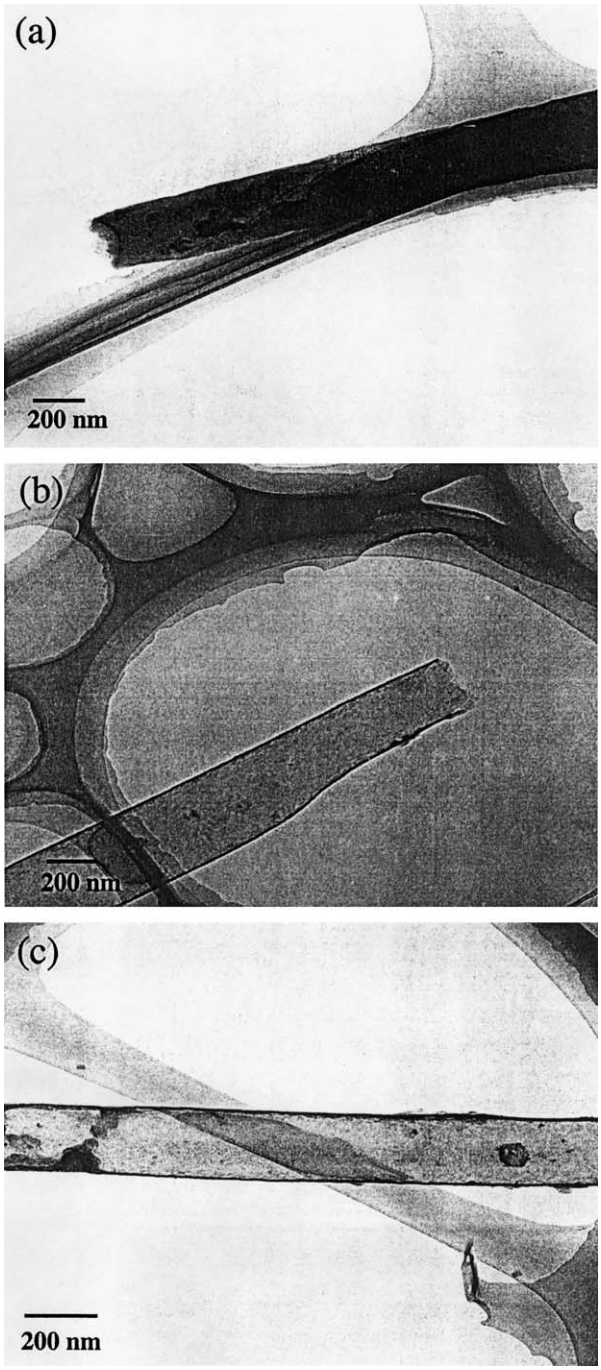

Fig. 6. HR-TEM images of carbon nanotube obtained by the carbonisation of polypyrrole at 1173 K for 4 h (a)–(c).

Fig. 1(a)–(d). Fig. 1(a) and (b) (at different magnification) shows the uniform pores present in the membrane. Fig. 1(c) and (d) (at different magnification) shows the uniform channels along the membrane. The pores and channels of the membrane have been effectively utilised for the polymerisation and subsequent carbonisation for the formation of the carbon nanotubes.

The scanning electron micrographs (SEM) of the carbon material obtained after the carbonisation of polypyrrole for 3 h at 973 and 1023 K (after the dissolution of the template) are shown in Fig. 2(a) and (b). It is evident from the micrographs, that the carbonisation time and temperature are not sufficient for the carbon material to be observed in the tubular form. So, the temperature of the carbonisation was increased to 1073 K and the time was varied between 3 and 5 h. Though Fig. 3(a)–(c) shows the carbon material in tubular form, the density of the tubular material was not found to be high.

The quality of carbon material obtained after the carbonisation at 1173 K for 3, 4, and 6 h are shown in Fig. 4(a)–(c), respectively. As it is evident from the micrographs (Fig. 4(a) and (b)), the carbonisation done for 3 and 4 h at 1173 K yielded tubular carbon material projecting perpendicularly from the surface of the SEM sample holder. But, as the carbonisation time is increased from 4 to 6 h, the tubular material slowly transforms into fibrillar material which is evident from Fig. 4(c).

3.2. Morphological characterisation of loaded and unloaded CNTs by HR-TEM

The HR-TEM of carbon nanotube obtained by the carbonisation of polypyrrole at 1173 K for 3 and 6 h are shown in Fig. 5(a)–(d). Though, the monodisperse cylindrical tube can be seen from Fig. 5(a), the tubules shown in Fig. 5(b)–(d) are not uniform. The HR-TEM of carbon nanotube obtained by the carbonisation of polypyrrole at 1173 K for 4 h are shown in Fig. 6(a)–(c). Fig. 6(a) clearly shows the open end of the tube and the outer diameter of the nanotube closely matches with the pore diameter of template used. Fig. 6(b) and (c) shows the hollow cylindrical nanotube and the open end of the nanotube could be utilised to load the nanoparticles. The transparent tube shown in Fig. 6(b) and (c) indicates the wall thickness of the tube is thin. Though, the carbon nanotube produced by this method are not completely graphitic in nature as produced by the arc discharge process, their disordered structure is quite typical of fibres or the nanotube produced by the decomposition of hydrocarbon [26].

The HR-TEM of Pt (Fig. 7(a)), Pt–Ru (Fig. 7(b) and (c)) and Pt–WO_3 (Fig. 7(d)) filled carbon nanotubes reflects that the particles are highly dispersed with particle size of 1.2 nm for Pt, 1.6–2 nm for Pt–Ru and 5 nm for Pt–WO_3.

3.3. Electrochemical behaviour of carbon materials

Fig. 8(a) shows the cyclic voltammogram of CNT–Nafion coated glassy carbon (GC) in 1 M H_2SO_4 scanned between −0.2 and +0.8 V vs. Ag/AgCl at a scan rate of 50 mV/s. The corresponding voltammogram obtained with plain Vulcan XC72R carbon, Graphite and Glassy Carbon (GC) electrodes are shown in Fig. 8(b)–(d). It is clear from the voltammogram that the GC/CNT–Nafion electrode shows higher current response than all the other electrodes with the same geometric area. Since the carbonaceous solid

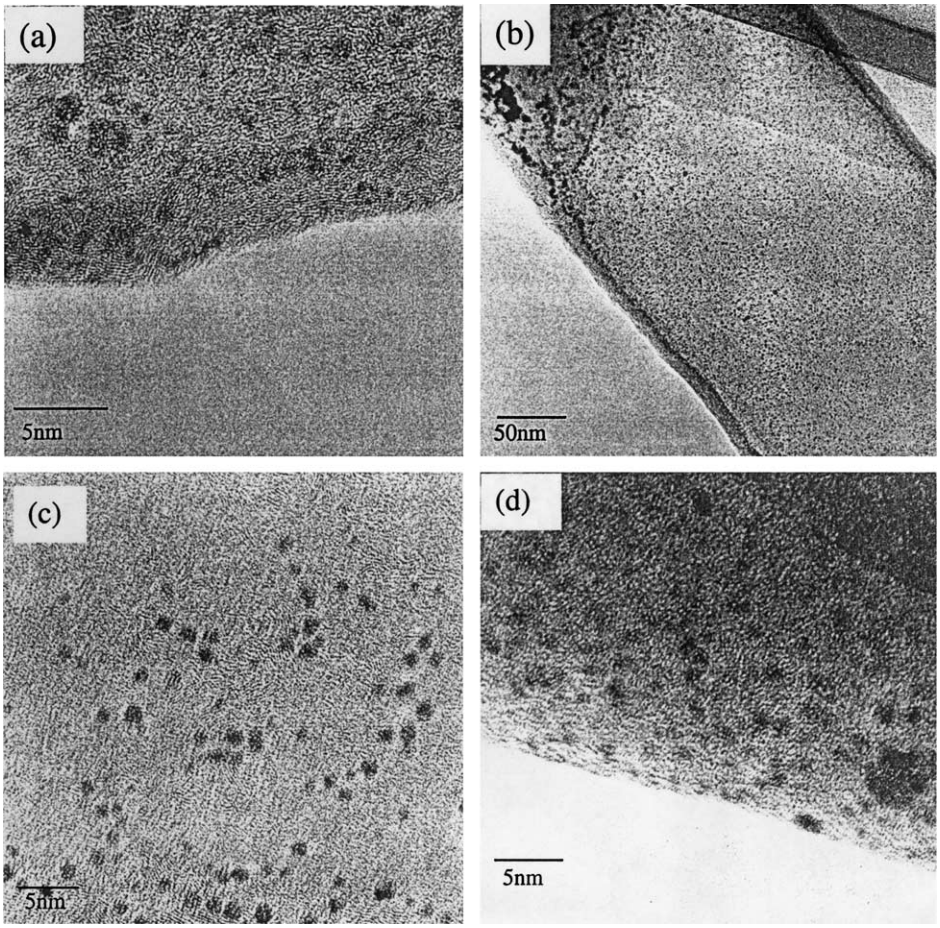

Fig. 7. HR-TEM images of loaded carbon nanotubes obtained by the carbonisation of polypyrrole at 1173 K for 4 h (a) Pt loaded CNT (b) and (c) Pt–Ru loaded CNT and (d) Pt–WO_3 loaded CNT.

is in the crystalline form of carbon, the higher available electroactive surface area was effectively utilised which is reflected from the higher electrochemical current response of Glassy carbon /CNT–Nafion electrode. In order to account for the higher current response, the electroactive surface of CNT, VulcanXC72, GC has been evaluated from cyclic voltammogram. The voltammogram was run in 5 mM $K_4[Fe(CN)_6]$ (probe molecule) in 0.1 M KCl at a scan rate of 50 mV/s. The typical voltammogram obtained with the GC/CNT–Nafion electrode is shown in Fig. 9. The well defined peak obtained at +0.3 and +0.15 V in the forward and the reverse scan is due to the Fe^{3+}/Fe^{2+} redox couple on GC/CNT–Nafion electrode. The electrochemical surface area has been evaluated from the peak current and by using the diffusion coefficient of $K_4[Fe(CN)_6]$ which is 0.76×10^{-5} cm^2/s in Randel Sevcik equation ($I_p = 2.69 \times 10^5 A D^{1/2} n^{3/2} \gamma^{1/2} C$). The electroactive surface area was found to be 0.25, 0.079, and 0.013 cm^2 for GC/CNT–Nafion, GC/Vulcan XC72R carbon–Nafion and plain GC electrodes, respectively. From these values it is clear that the tubular morphology favours the higher electroactive surface area of the carbon nanotube based electrode.

3.4. Surface characterisation of loaded carbon nanotubes by XPS

The X-ray photoelectron spectra (not shown) of Pt 4f with peak binding energy of 71.2 eV ($4f_{7/2}$) and 74.6 eV ($4f_{5/2}$) suggests that the Pt particles are present in the metallic state. The peak binding of Pt $4f_{7/2}$ at 71.4 eV and Pt $4f_{5/2}$ at 74.5 eV shows that the Pt ions are completely reduced (Fig. 10(a)) in the Pt–Ru loaded carbon nanotube. Though the Ru 3d signal is obscured by C1s signal, the deconvoluted spectra (Fig. 10(b)) shows the peak binding energies of Ru $3d_{5/2}$ at 280.6 eV and Ru $3d_{3/2}$ at 284.8 eV suggesting that the Ru particles are also in the zero valent state. Similarly, the peak with binding energies of Pt 4f centred at 71.2 eV of Pt $4f_{7/2}$ and 74.4 eV of Pt $4f_{5/2}$ (Fig. 10(c)) revealed that the Pt is in the zero valent state in Pt–WO_3 loaded carbon nanotube. The X-ray photoelectron spectra of W (Fig. 10(d)) shows a doublet with peak binding energies centred at 35.8 eV of W ($4f_{7/2}$) and 38.5 eV of W ($4f_{5/2}$), respectively. This suggests that W may be in the +VI oxidation state.

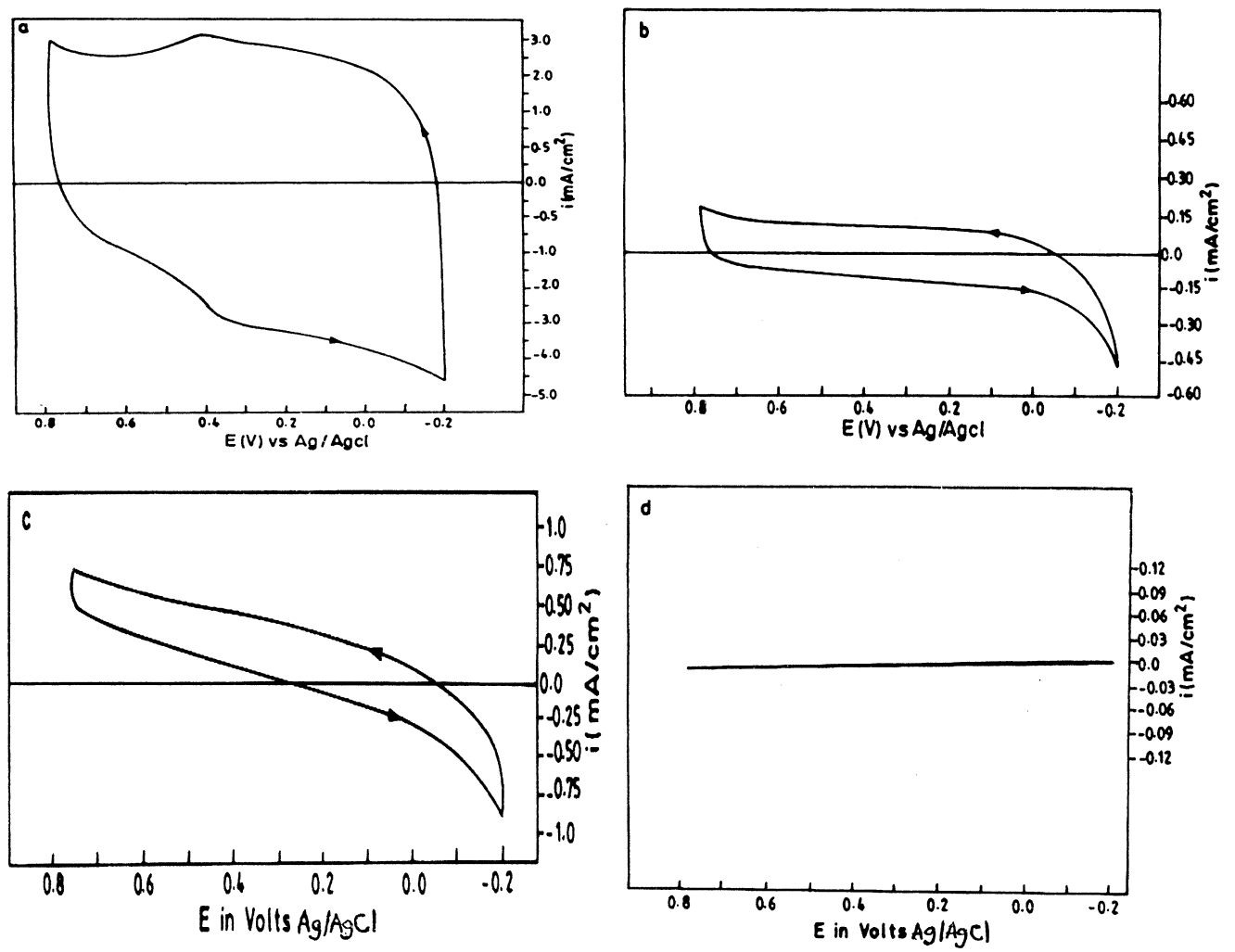

Fig. 8. Cyclic voltammetric response of carbon nanotube electrode in comparison with electrodes based on other carbon material The voltammogram was run in 1 M H_2SO_4 at 50 mV/s between −0.2 and +0.8 V vs. Ag/AgCl.

3.5. Electrochemical behaviour of WO_3 loaded CNTs

The cyclic voltammogram of GC/CNT–WO_3–Nafion electrode run in 1 M H_2SO_4 at different scan rates is shown in Fig. 11(a), the potential was scanned between −0.4 and +0.74 V vs. Ag/AgCl. The electrochemical response due to W is seen at −0.1 V in the forward scan, which clearly matches with the peak reported in the literature [31]. The cyclic voltammogram of Nafion coated on Glassy carbon (GC) electrode in 1 M H_2SO_4 run at 50 mV/s is shown in Fig. 11(b) for comparison. The absence of any peak between −0.8 and +0.8 V clearly demonstrates that the response obtained in Fig. 11(a) is due to W.

3.6. Evaluation of methanol electrooxidation activity of composite materials

The cyclic voltammogram of GC/CNT–Pt–Nafion electrode in 1 M H_2SO_4 (in the absence of methanol) scanned between −0.2 and +0.8 V and run at 50 mV/s is shown in Fig. 12(a). A broad peak at −0.1 V is due to the hydrogen adsorption on Pt. The cyclic voltammogram of GC/CNT–Pt–Nafion electrode in 1 M H_2SO_4/1 M CH_3OH run at 50 mV/s is shown in Fig. 12(b). The onset of methanol oxidation starts around +0.2 V and peaks at +0.65 V with a peak current density of 14 mA/cm^2 and in the reverse scan another oxidation peak appears at +0.55 V. The decrease in the peak current in the reverse scan, suggest the poisoning of the electrode surface due to the strongly adsorbed intermediate as suggested by other authors [12]. The cyclic voltammogram of GC/CNT–Pt–WO_3–Nafion electrode run under the same conditions in the presence of methanol is shown in Fig. 12(c). The onset of methanol oxidation starts around +0.1 V in the forward scan and relatively high current density (98.5 mA/cm^2) at +0.7 V vs. Ag/AgCl was obtained at room temperature and nearly no poisoning phenomenon occurs as observed by the higher current obtained in the reverse scan. The carbon

Table 1
Co-relation of catalytic activity of GC/CNT–Pt–WO_3–Nafion electrode for methanol oxidation with percentage of nitrogen in the carbon nanotube

S. No.	Percentage of nitrogen (%)	Activity[a] (mA/cm^2)
1	3	80.5
2	3–8	80.5–98.5
3	10	75.5

[a] Activity evaluation was based on the maximum current obtanied in the cyclic voltammogram which was run between −0.2 and +0.8 V vs. Ag/AgCl at 50 mV/s in 1 M H_2SO_4/1 M CH_3OH.

nanotubes obtained at 1173 K for 4 h was used as the electrode for the CNT based materials.

3.7. Effect of nitrogen content in the CNT on catalytic activity of methanol oxidation

In order to see the effect of the nitrogen content in the carbon nanotube, the catalytic activity was evaluated by increasing the percentage of nitrogen in the carbon nanotube from 3 to 10% (the variation of the nitrogen content has been done by fixing the temperature at 1173 K and varying the carbonisation time between 2.30 and 6 h.). It is evident from Table 1, the catalytic activity for methanol oxidation increases from 80.5 to 98.5 mA/cm^2, when the nitrogen content increases from 3 to 8%. There is a decrease in the catalytic activity, when the nitrogen content is increased to 10%. Table 1, shows the catalytic activity of GC/CNT–Pt–WO_3–Nafion electrode for methanol oxidation which was evaluated from cyclic voltammogram run at 50 mV/s in 1 M H_2SO_4/1 M CH_3OH between −0.2 and +0.8 V. The maximum current obtained per unit area observed in the forward sweep has been tabulated in Table 1. The nitrogen when it is present in the optimum amount could have helped for the better dispersion of the catalytic nanoparticles. This could be one of the reasons for the observed higher activity.

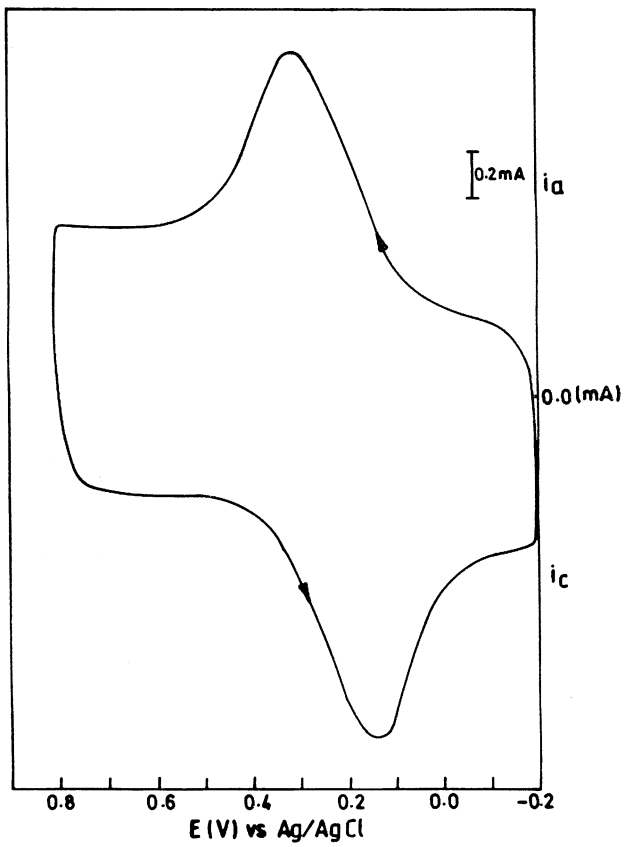

Fig. 9. Typical cyclic voltammogram of GC/CNT–Nafion electrode in 5 mM $K_4[Fe(CN)_6]$/0.1 M KCl run at 50 mV/s between −0.2 and +0.8 V vs. Ag/AgCl.

The amount of Pt was found to be 16.5 μg for GC/CNT–Pt–WO_3–Nafion, 22 μg for GC/CNT–Pt–Nafion, 37 μg for GC/20% Pt–Ru E-TEK–Nafion/Vulcan Carbon and 40 μg GC/20% Pt E-TEK–Nafion/Vulcan Carbon and the nitrogen content in the nanotube was 8%.

3.8. Chronoamperometric response of composite electrodes for methanol oxidation

Fig. 13 shows the chronoamperometric response of different electrodes for methanol oxidation at +0.6 V in 1 M H_2SO_4/1 M CH_3OH for 2 h. It is clear from Fig. 13(a), that there is a decay in the current with respect to time for GC/CNT–Pt–WO_3–Nafion electrode for methanol oxidation which is not truly reflected in the cyclic voltammogram (Fig. 12(c)). This is because of the lower time scale of the cyclic voltammetric experiment. But, still when the electrodes are compared under identical experimental conditions, the GC/CNT–Pt–WO_3–Nafion shows a better activity and stability to the GC/CNT–Pt–Nafion (Fig. 13(c)), GC/E-Tek 20% Pt/Vulcan XC72 carbon–Nafion (Fig. 13(d)) and bulk platinum electrodes (Fig. 13(e)). Though GC/E-Tek 20% Pt–Ru/Vulcan XC72 carbon–Nafion (Fig. 13(b)) shows lower activity (35.7 mA/cm^2 after 20 min) as compared to GC/CNT–Pt–WO_3–Nafion (50 mA/cm^2 after 20 min) (Fig. 13(a)), the stability of the former is better as it is evident from Fig. 13(a) and (b). The higher activity of the carbon nanotubes (synthesised at 1173 K, for 4 h) based electrodes demonstrates the better utilisation of the catalyst. The increased utilisation is mainly due to the tubular morphology of the carbon, which allows the particle to be highly dispersed (as revealed by Fig. 3), which result in lower particle size. The lower stability of GC/CNT–Pt–WO_3–Nafion electrode as compared to GC/E-Tek 20% Pt–Ru/Vulcan XC72 carbon–Nafion electrode might be due to the slow dissolution of tungsten from the electrode upon constant electrolysis. The lower activity of GC/E-Tek 20% Pt/Vulcan XC72 carbon–Nafion electrode might be due to the poor utilisation and increase in internal resistance offered by the Nafion which is a poor electronic conductor. Though Nafion is used as a binder in the CNT

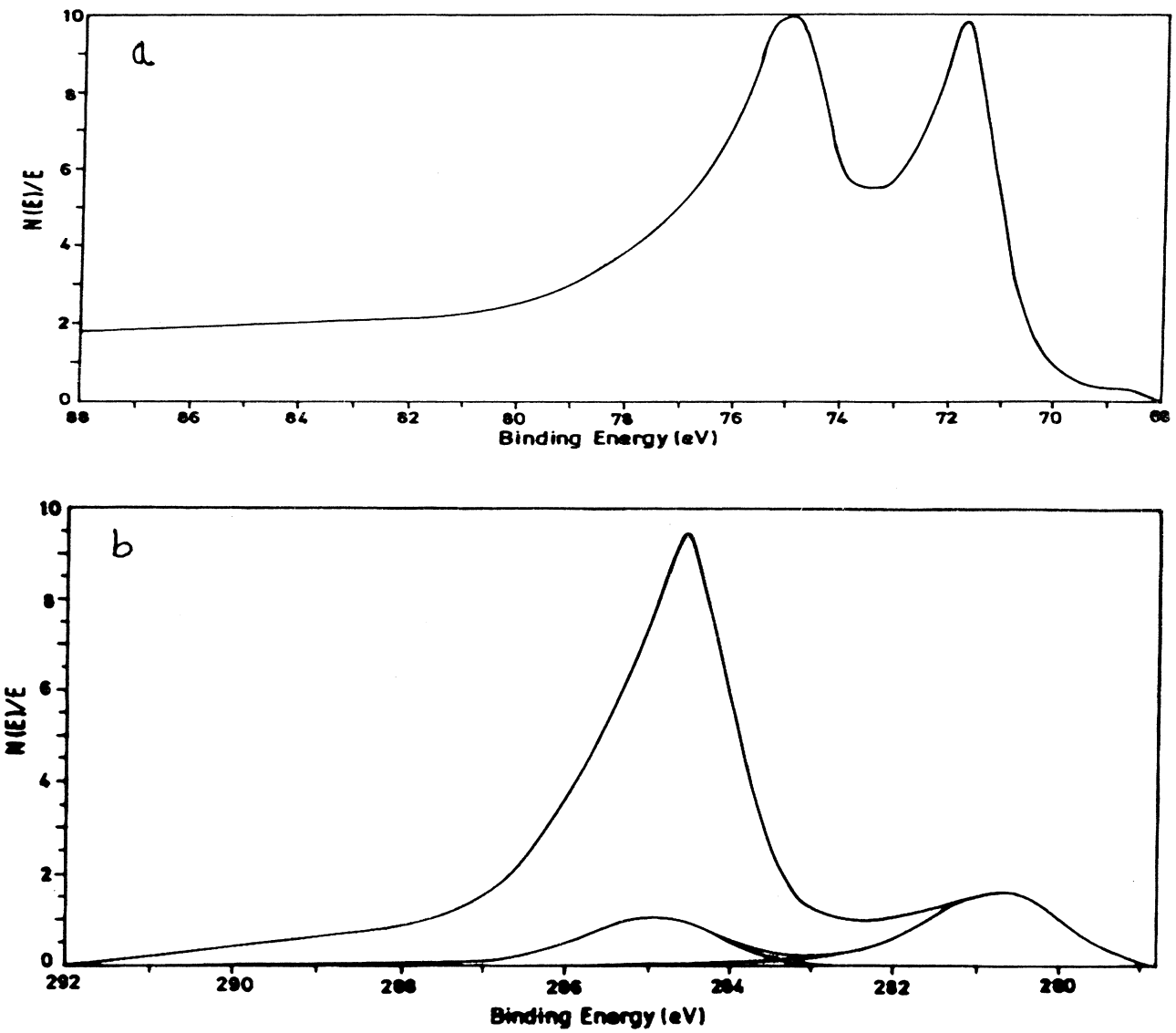

Fig. 10. XPS of (a) Pt 4f in Pt–Ru loaded CNT (b) Ru 3d in Pt–Ru loaded CNT (also shown C1s of Pt–Ru loaded CNT in (b)), (c) Pt 4f in Pt–WO_3 loaded CNT, and (d) W 4f in Pt–WO_3 loaded CNT.

based electrodes as well, the tubular morphology would have favoured the higher activity and stability.

It is well known that ash-free activated carbon obtained at high temperatures (>973 K) possess a relatively hydrophobic surface [32]. But, the presence of functional group on the surface of the activated carbon can also have a substantial effect on their adsorption properties. In particular a small amount of oxygen containing groups give rise to hydrophilic centres [33]. It was shown [34] that the carbonisation of nitrogen containing polymer precursor yields carbon residue with N and O-containing functional groups. These functionalities make the surface hydrophilic. It was proposed [13] that the catalyst should be partly oxophilic (hydrophilic) to remove the carbonaceous residues during the methanol oxidation. In the present case, the nitrogen present in the carbon nanotube could have increased the oxophilic centres due to their partly hydrophilic nature. This might be the reason for the increased activity and stability.

The activity and the stability of the catalyst for methanol oxidation (from Fig. 13) decreases in the following order: GC/CNT–Pt–WO_3–Nafion > GC/Pt–Ru E-TEK 20%/VulcanCarbon–Nafion > GC/CNT–Pt–Nafion > GC/E-TEK 20% Pt/Vulcan carbon–Nafion > Bulk Pt.

In order to compare the stability of Pt–WO_3 loaded carbon nanotube (8% nitrogen) with the Pt–Ru loaded carbon nanotube (8% nitrogen), the catalytic activity was evaluated by polarising the electrode at +0.4 V vs. Ag/AgCl in 1 M H_2SO_4/1 M CH_3OH for 2 h, as it is evident from Fig. 14(a), the GC/CNT–Pt–WO_3–Nafion electrode

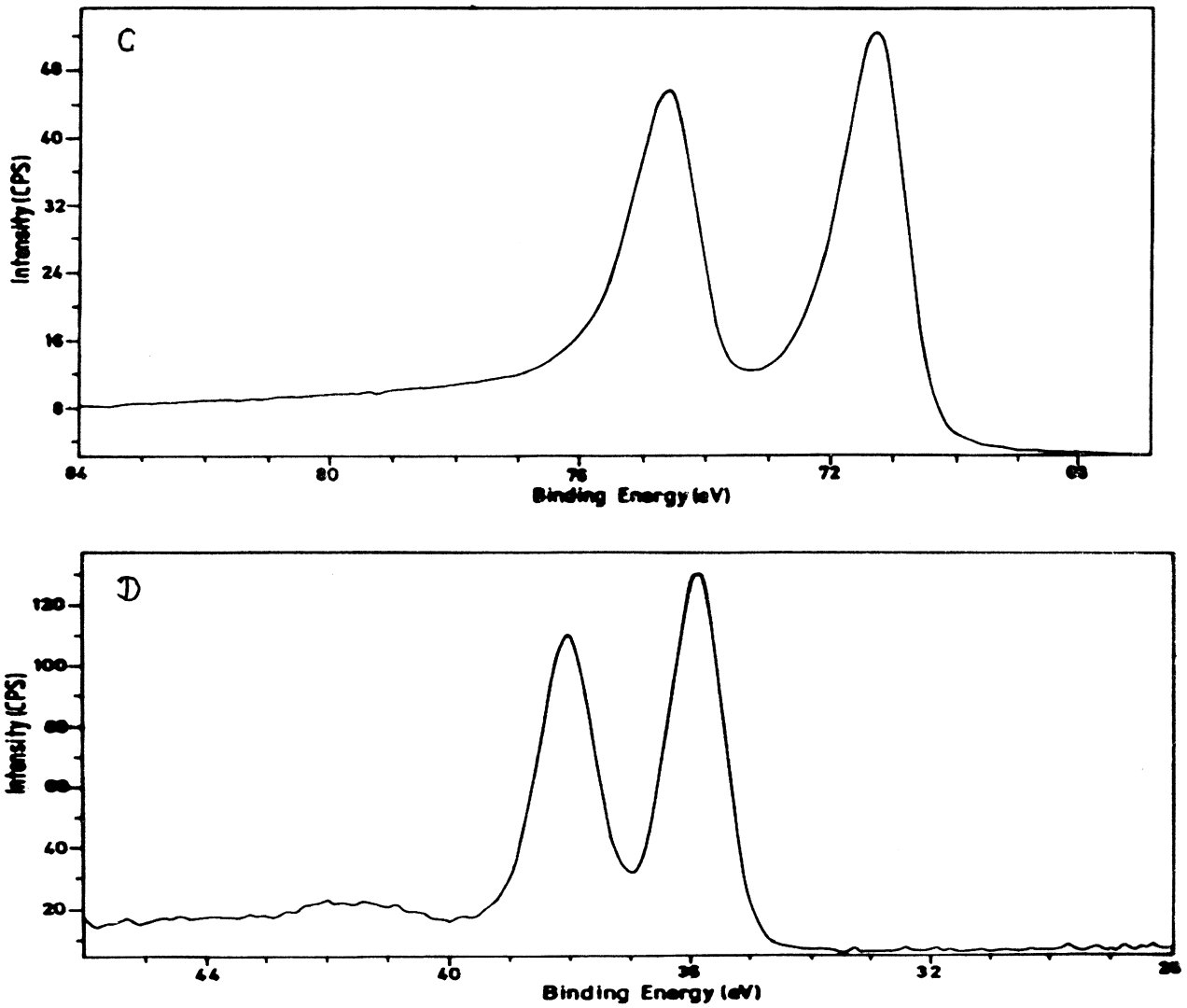

Fig. 10 (*continued*)

not only showed higher initial activity but also is more stable than GC/CNT–Pt–Ru electrode (Fig. 14(b)). The probable reason could be the lower polarisation potential. At this potential, the leaching of W would not have had a pronounced effect on the stability of the electrode for methanol oxidation.

4. Conclusions

The template aided synthesis of carbon nanotube using polypyrrole precursor yielded well-aligned carbon nanotubes and nanofibres. The higher electrochemical response of the carbon nanotube as compared to the Vulcan XC72R carbon, Graphite and GC electrode shows the higher available electroactive surface area (as evaluated from the cyclic voltammetry). The open end of the carbon nanotube (as revealed from HR-TEM) has been effectively utilised to load the catalytic nanoparticles. The catalytic nanoparticles are effectively dispersed inside the tube with the particle size of around 1.2, 2, and 5 nm for Pt, Pt–Ru, and Pt–WO_3, respectively. The XPS showed the presence of Pt and Ru in the metallic state and W in +VI oxidation state. The higher activity of GC/CNT–Pt–WO_3–Nafion and GC/CNT/Pt–Nafion compared to that of commercial Pt and Pt–Ru catalyst suggests, that the higher electrochemical surface area of the carbon nanotube has been effectively utilised for the dispersion of catalytic nanoparticles which results in the higher activity for methanol oxidation. The higher activity of GC/CNT/Pt–WO_3–Nafion over GC/CNT/Pt–Nafion suggests that the bifunctional mechanism is operative.

The activity for methanol oxidation is altered, when the nitrogen content in the carbon nanotube is altered. The nitrogen and oxygen functionalities in the carbon nanotube not only help in the better dispersion of the catalytic particles but also alter the hydrophilicity of the carbon

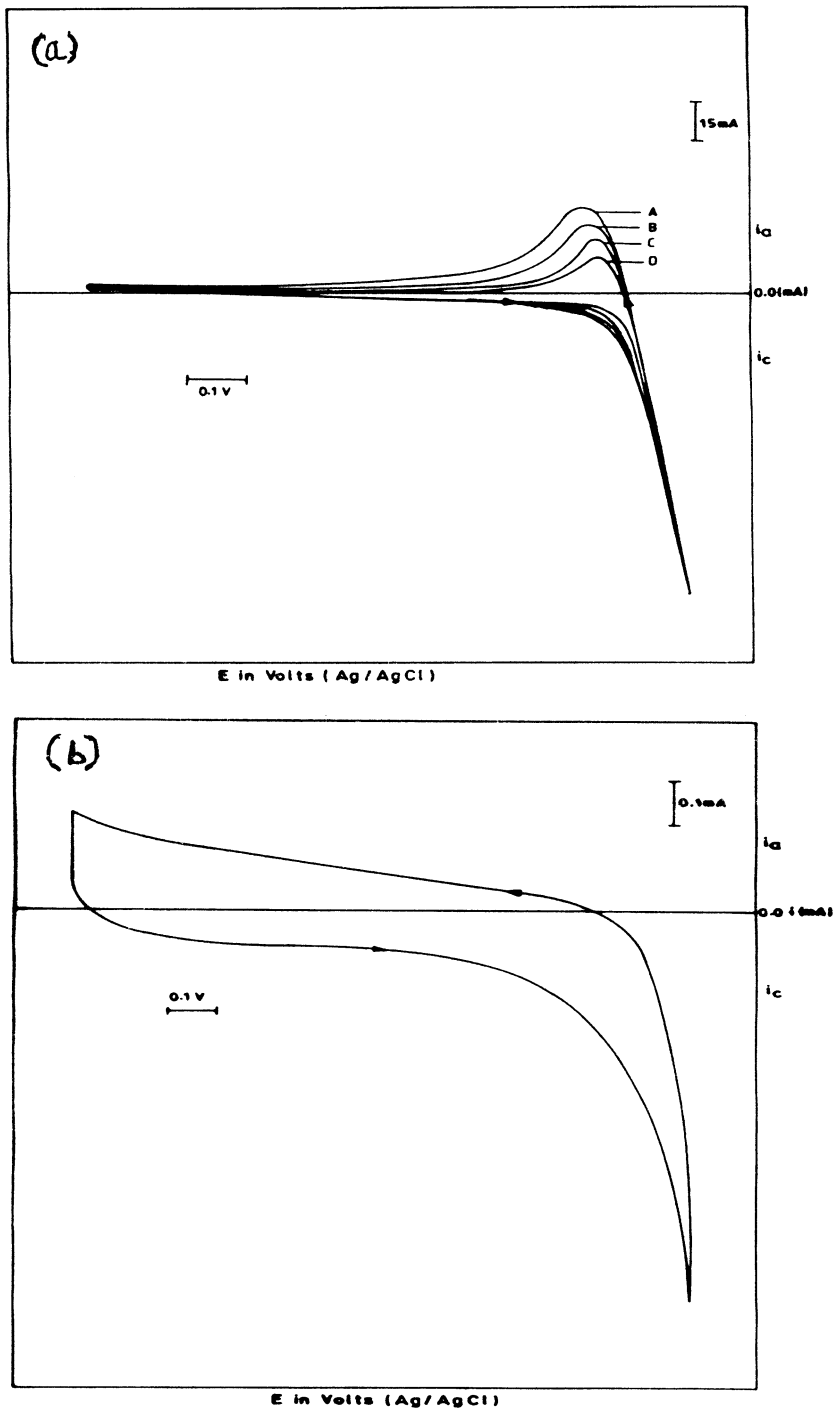

Fig. 11. Cyclic voltammetric response of (a) GC/CNT–WO_3–Nafion and (b) GC/Nafion electrodes in 1 M H_2SO_4 at 50 mV/s between −0.8 and +0.8 V vs. Ag/AgCl.

nanotube. The probable alteration in the hydrophilicity of the carbon nanotube might be one of the reasons for the better stability of the carbon nanotube based electrodes. The activity and the stability of the methanol oxidation follows the order: GC/CNT–Pt–WO_3–Nafion > GC/Pt–Ru E-TEK 20%/VulcanCarbon–Nafion > GC/CNT–Pt–Nafion > GC/E-TEK 20% Pt/Vulcan carbon–Nafion > Bulk Pt. But though the activity of E-TEK Pt–Ru catalyst is lower than that of GC/CNT–Pt–WO_3–Nafion, the stability of the latter is slightly lower probably due to the dissolution of tungsten from the electrode on prolonged electrolysis at +0.6 V. The higher activity and stability for methanol oxidation of GC/CNT–Pt–WO_3–Nafion electrode compared to GC/CNT–Pt–Ru–Nafion electrode

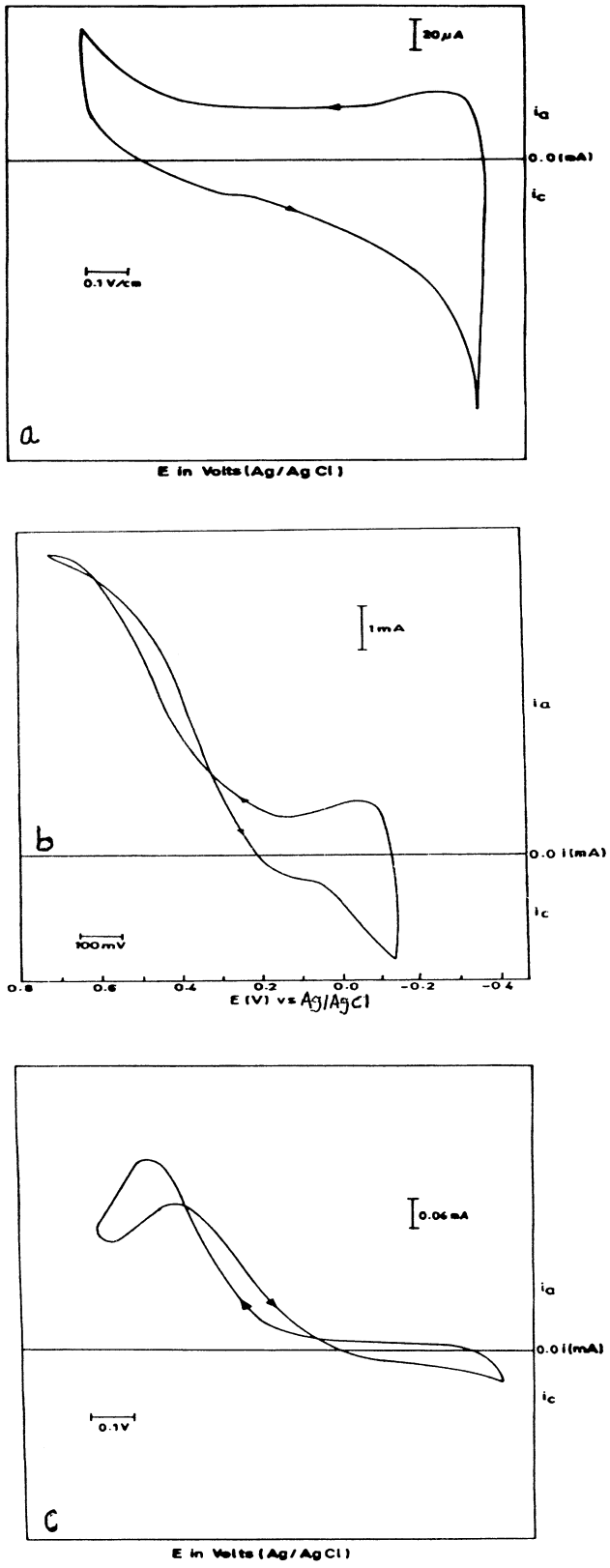

Fig. 12. Cyclic voltammogram of (a) GC/CNT–Pt–Nafion in 1 M H_2SO_4 (absence of methanol), (b) GC/CNT–Pt–WO_3–Nafion, and (c) GC/CNT–Pt–Nafion electrodes in 1 M H_2SO_4/1 M CH_3OH run at 50 mV/s between −0.2 and +0.8 V vs. Ag/AgCl. The nitrogen content in the nanotube was 8%.

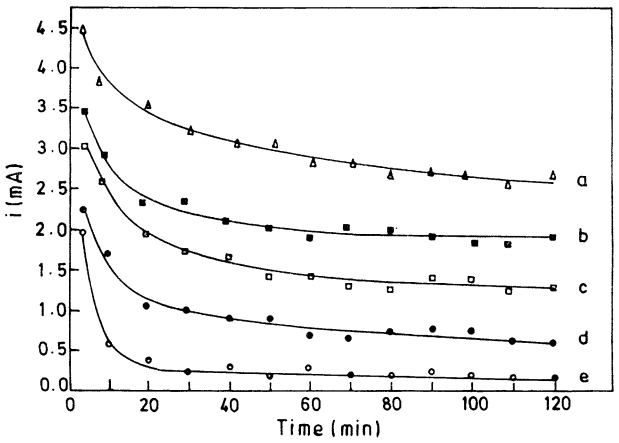

Fig. 13. Chronoamperometric response of (a) GC/CNT–Pt–WO_3–Nafion, (b) GC/E-TEK 20% Pt–Ru/Vulcan carbon–Nafion, (c) GC/CNt–Pt–Nafion, (d) GC/E-TEK 20% Pt/Vulcan Carbon–Nafion, and (e) Bulk Pt electrodes polarised at +0.6 V vs. Ag/AgCl in 1 M H_2SO_4/1 M CH_3OH for 2 h. The nitrogen content in the nanotube was 8%.

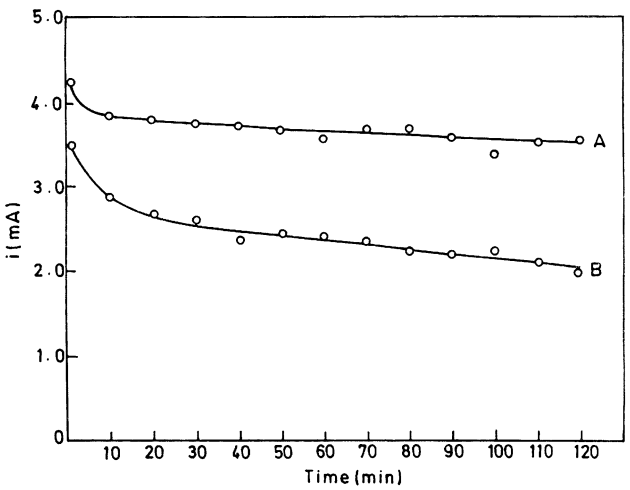

Fig. 14. Chronoamperometric response of (a) GC/CNT–Pt–WO_3–Nafion and (b) GC/CNT–Pt–Ru–Nafion electrodes polarised at +0.4 V vs. Ag/AgCl in 1 M H_2SO_4/1 M CH_3OH for 2 h. The nitrogen content in the nanotube was 8%.

polarised at +0.4 V probably suggests that the dissolution of W might not have pronounced effect on the methanol oxidation.

Acknowledgments

The authors sincerely thank the Head and Director, Prof. Michael Gratzel, Laboratoire de Photonique et Interfaces (LPI) for providing the laboratory facilities to carry out this work at Ecole Polytechnique Federale De Lausanne (EPFL), Switzerland. We thank Dr A.J. McEvoy, LPI, EPFL, Switzerland for the fruitful discussion we had with him over this work. We also thank the Centre Interdepartmental de Microscopic Electronique (CIME) at EPFL for access to Electron Microscopes. We thank the Department des

Materiaux (DMX) at EPFL, Switzerland for XPS measurements. Discussions with Mr N. Xanthopoulos, DMX, EPFL, Switzerland regarding XPS are also appreciated.

References

[1] Witham CK, Chun W, Valdez TI, Narayanan SR. Electrochem Solid-State Lett 2000;3:497.
[2] Jarvi TD, Stuve EM. In: Lipkowski J, Ross PN, editors. Electrocatalysis. New York: Wiley/VCH; 1988. p. 75.
[3] Parsons R, VanderNoot T. J Electroanal Chem 1988;257:1.
[4] Watanabe M, Motto S. J Electroanal Chem 1975;60:267.
[5] Haner AN, Ross PN. J Phys Chem 1991;95:3740.
[6] Gotz M, Wendt H. Electrochim Acta 1998;43:3637.
[7] Ley KL, Liu B, Pu C, Fan Q, Leyarovska N, Segre C, Smotkin ES. J Electrochem Soc 1997;144:1543.
[8] Aramata A, Masuda M. J Electrochem Soc 1991;138:1949.
[9] He C, Kunz HR, Fenton JM. J Electrochem Soc 1997;144:970.
[10] Arico AS, Poltarzoeski Z, Kim H, Morana A, Antonucci V. J Power Sour 1995;55:159.
[11] Reddington E, Sapienza A, Gurrau B, Viswanathan R, Sarangapani S, Smotkin ES, Mallouk TE. Science;280:1735.
[12] Shen PK, Tseung ACC. J Electrochem Soc 1994;4:1289.
[13] Mukerjee S, McBreen J. J Electrochem Soc 1999;146:600.
[14] Kuleza PJ, Faulkner LR. J Electrochem Soc 1989;136:707.
[15] Shukla AK, Hamnett A, Roy A, Barman SR, Sarma DD, Alderucci V, Pino L, Giordano N. J Electroanal Chem 1993;352:337.
[16] Blurton KF. Carbon 1972;10:305.
[17] Iijima S. Nature 1991;354:56.
[18] Bein T, Stucky GD. Chem Mater 1996;8:1569.
[19] Dai H, Wony EW, Leiber CM. Science 1996;272:523.
[20] Rodriguez NM, Kim MS, Baker RTK. J Phys Chem 1994;98:13108.
[21] Che G, Lakshmi BB, Martin CR, Fisher ER. Langmuir 1999;15:750.
[22] Baum RM. Chem Engng News 1997;75:39.
[23] Ago H, Komatsu T, Ohishima S, Kuriki Y, Yumura M. Appl Phys Lett 2001;77:79.
[24] Wu F, Liu H, Lan Y, Fan SS, Yuan HT, Song DY, Shen PW. Chem Phys Lett 2000;327:271.
[25] Che G, Lakshmi BB, Martin CR, Fisher ER. Langmuir 1999;15:750.
[26] Kyotani T, Tsai LF, Tomita A. Chem Mater 1995;7:1427.
[27] Ranjani VP, Phani KLN, Martin CR. Adv Mater 1995;7:896.
[28] Che G, Lakshmi BB, Martin CR, Fisher ER. Chem Mater 1998;10:260.
[29] Bessel CA, Laubernds K, Rodriguez NM, Baker RTK. J Phys Chem 2001;105:1115.
[30] Rajesh B, Ravindranathan Thampi K, Bonard J-M, Viswanthan B. J Mater Chem 2000;10:1757.
[31] Figlarz M. Prog Solid State Chem 1989;19:1.
[32] Puri BR. In: Walker PL, editor. Chemistry an physics of carbon, vol. 6. New York: Marcel Decker; 1970. p. 191.
[33] Rivera-Utrilla J, Ferro-Garcia MA. Adsorption Sci Technol 1986;3:293.
[34] Wang Z, Lu Z, Huang X, Xue R, Chen L. Carbon 1998;36:51.